

First-Return Statistics in Henyey–Greenstein Scattering: Motzkin Polynomials and the Cauchy Kernel

C Zeller¹ and R Cordery²

¹Claude Zeller Consulting LLC, Tillamook, Oregon 97134, USA

²Department of Physics, Fairfield University, Fairfield, Connecticut 06824, USA

czeller@ieee.org, rcordery@fairfield.edu

Abstract

In our previous work, we showed that first-return probabilities in one-dimensional scattering expand naturally in Catalan and Motzkin numbers. Extending this framework to three-dimensional Henyey–Greenstein scattering requires correcting for the restricted angular phase space imposed by a boundary. We introduce a Boundary Truncation Factor (BTF) that modifies the effective anisotropy coefficient governing first return. Extensive Monte Carlo simulations (approximately 10^{12} scattering events) reveal that the BTF follows a remarkably simple Cauchy kernel in the scattering order n , with width $m^*(g) = 4g/(1-g)$, amplitude $A(g) = 1 - g(1+g)/2$, and a peak at the minimum return order $n = 2$. This closed-form expression reproduces Monte Carlo results to 1–2% accuracy for $g < 2/3$ across the full range $n = 2$ –100, and can be extended to higher anisotropy using a one-parameter modified Cauchy kernel. While a first-principles derivation of the kernel remains open, the empirical law provides a compact and computationally efficient replacement for brute-force Monte Carlo in inverse and iterative transport problems.

Keywords: first-passage problem, random walk, Cauchy kernel, Motzkin polynomials, radiative transfer, Henyey–Greenstein scattering

1 Introduction

First-passage problems appear throughout statistical mechanics—in polymer physics, diffusion-limited aggregation, financial mathematics, and queueing theory [1, 2, 3]. A clean example arises in radiative transport: photons entering a scattering medium execute a three-dimensional random walk and may return to the entry boundary. The statistics of this first-passage event encode how stochastic motion interacts with geometric constraint.

Throughout, “first-return” means first passage back to $z = 0$ from $z > 0$ with negative z -velocity—the photon must exit, not graze inward.

In our previous work in this journal [6], we established that first-return probabilities in one-dimensional isotropic scattering expand in Catalan numbers, the combinatorial objects

counting Dyck paths. The reflectance of a semi-infinite Kubelka–Munk medium [8] admits the generating function representation

$$R_\infty(S, \chi) = \frac{1}{2} \cdot \frac{S}{S + \chi} \cdot C \left(\frac{S^2}{4(S + \chi)^2} \right) \quad (1)$$

where $C(x) = \sum_{n=0}^{\infty} C_n x^n$ is the Catalan generating function [18] and $C_n = (2n)!/(n!(n+1)!)$. This is distribution-free: it depends only on the zigzag structure, not step lengths. Forward-peaked scattering introduces “flat” steps—events preserving the sign of z -velocity. The Motzkin extension [15, 16] handles this, giving

$$P_{\text{refl}}^{(1D)}(n, r) = M_{n-2} \left(\frac{1-2r}{r} \right) \cdot \left(\frac{r}{2} \right)^{n-1} \quad (2)$$

where $M_n(t)$ is the Motzkin polynomial and r the backward-step probability.

The central challenge is extending this framework to *three-dimensional anisotropic* scattering governed by the Henyey–Greenstein phase function [13]. Direct embedding of Motzkin structure via an effective backscattering coefficient $r_b(g)$ fails; Monte Carlo studies [7] show the mapping requires a **Boundary Truncation Factor** (BTF) that accounts for geometric constraints at the boundary.

We show that the BTF follows a **Cauchy kernel** in the scattering order n :

$$\text{BTF}(n, g) = \frac{A(g)}{1 + \left(\frac{n-n_0}{m_\star(g)} \right)^2} \quad (3)$$

with parameters expressible in terms of the anisotropy factor g alone:

$$m_\star(g) = \frac{4g}{1-g} \quad (\text{width}) \quad (4)$$

$$A(g) = 1 - \frac{g(1+g)}{2} \quad (\text{amplitude}) \quad (5)$$

$$n_0 = 2 \quad (\text{peak location}) \quad (6)$$

The simple integer coefficients suggest underlying geometric structure; however, a first-principles derivation of the Cauchy form remains an open problem (Section ??).

The theory applies for $g \lesssim 2/3$ and $n \geq 2$; above $g \approx 2/3$, deviations grow gradually but can be corrected by a modified Cauchy kernel with a shape parameter (Section 7).

Practical scope of the validity range. The constraint $g < 2/3$ complements rather than competes with biological tissue optics, where $g \approx 0.9$ –0.98 is typical [22]. Table 1 summarizes representative anisotropy factors for various scattering media. Many industrial and environmental applications fall within the validity range of the present theory; for higher-anisotropy materials, the Cauchy kernel form remains valid but parameters benefit from Monte Carlo calibration (Section 4).

1.1 Relation to previous work

Table 2 summarizes the progression from [6].

Table 1: Representative anisotropy factors g for various scattering media. Values marked with \dagger require verification.

Material	g	Reference
<i>Within validity range ($g < 2/3$)</i>		
Isotropic scatterers	0	Definition
Paper / print media	0.4–0.6 †	[23]
<i>Above validity range ($g > 2/3$)</i>		
Human dermis/epidermis	0.7–0.9	[21]
Biological tissue (in vivo)	0.9–0.98	[22]
Intralipid phantoms	~ 0.9	Standard value

Table 2: Progression of results from [6] through the present work.

Aspect	Zeller & Cordery (2020)	Present work
Dimension	1D	$3D \rightarrow 1D$ via BTF
Scattering	Isotropic + forward bias	Henyey–Greenstein
Combinatorics	Catalan \rightarrow Motzkin	Motzkin + BTF correction
BTF	Not needed	Cauchy kernel (empirical)
Incidence	Normal only	Normal + oblique
Validity range	—	$g < 2/3$ (Cauchy); $g < 0.95$ (modified)
Status	Derived	Empirical; derivation open

From our 2020 paper, we carry forward: (i) the Motzkin polynomial framework (equation (2)); (ii) the distribution-free character of first-passage combinatorics; and (iii) the connection to classical fluctuation theory [5, 4]. What is new here is: (i) identification of the Cauchy kernel form for the BTF through systematic model selection; (ii) determination of the parameters $m_*(g)$ and $A(g)$ from Monte Carlo fitting; (iii) generalization to oblique incidence via Motzkin polynomials with transverse activity; and (iv) a modified Cauchy kernel extending validity to high anisotropy.

1.2 Comparison with generalized Kubelka–Munk

Our approach differs from previous 3D extensions of Kubelka–Munk. Sandoval and Kim [10, 11] extended KM through double spherical harmonics (DP_1), obtaining an 8×8 system for forward and backward power flow. For isotropic scattering in optically thick media, their generalized KM achieves errors below 15% when $z_0 \geq 10$ (where z_0 is the optical thickness).

However, DP_1 encounters difficulties for anisotropic scattering. Its basis functions contain only first-order azimuthal harmonics and cannot capture forward-peaked phase functions. At $g = 0.8$, Sandoval and Kim found errors exceeding 80% in transmitted power; at higher anisotropy, the approximation gives negative intensities.

The BTF framework inverts the dimensional strategy: instead of enriching 1D equations with 3D coupling, we use 1D combinatorics and correct for boundary truncation. Table 3 compares the two approaches.

Table 3: Comparison of dimensional reduction strategies for semi-infinite media.

Property	gKM (Sandoval & Kim)	BTF (this work)
Geometry	Finite slab	Semi-infinite
Strategy	$1D \rightarrow 3D$ extension	$3D \rightarrow 1D$ reduction
Angular basis	DP_1 (4 func./hemisphere)	HG sampling + Motzkin
Isotropic limit	<15% error for $z_0 \geq 10$	Recovers Catalan structure
Anisotropic range	$g \lesssim 0.5$ (qualitative)	$g < 2/3$ (<2% deviation)
High- g behavior	Unphysical (negative values)	Predictable drift
Incidence	Oblique via eigenmode	Oblique via Motzkin extension
Computational form	8×8 PDE system	1D polynomial evaluation

Practitioner guidance. For semi-infinite media with $g \lesssim 2/3$, BTF+Motzkin beats DP_1 : 1D polynomial evaluation achieves sub-2% accuracy versus 15%+ for gKM. For finite slabs or strong absorption, use gKM or Monte Carlo. BTF excels in inverse problems requiring thousands of transport evaluations.

1.3 Paper organization

Section 2 reviews the 1D Motzkin framework [6]. Section 3 introduces the Boundary Truncation Factor and its Cauchy kernel form. Section 4 describes Monte Carlo validation. Section 5 presents the computational algorithm. Section 6 extends the framework to oblique

incidence. Section 7 presents the modified Cauchy kernel for high-anisotropy scattering ($g > 2/3$). Section 8 concludes.

2 One-dimensional theory: Catalan and Motzkin structures

We review results from [6]; see [1, 2] for background.

2.1 Kubelka–Munk reflectance and Catalan numbers

The Kubelka–Munk equations [8, 12] describe one-dimensional radiative transport with isotropic scattering:

$$\begin{pmatrix} dI \\ dJ \end{pmatrix} = \begin{pmatrix} -(S + \chi) & S \\ -S & (S + \chi) \end{pmatrix} \begin{pmatrix} I \\ J \end{pmatrix} dz \quad (7)$$

where I and J are forward and backward fluxes, S the scattering coefficient, and χ the absorption coefficient. The reflectance of a semi-infinite slab is

$$R_\infty(S, \chi) = \frac{S + \chi}{S} - \sqrt{\left(\frac{S + \chi}{S}\right)^2 - 1} \quad (8)$$

The key result of [6] is that this reflectance expands in Catalan numbers:

$$R_\infty(S, \chi) = \sum_{n_p=1}^{\infty} \frac{C_{n_p-1}}{2^{2n_p-1}} \left(\frac{S}{S + \chi}\right)^{2n_p-1} \quad (9)$$

Photon trajectories form zigzag random walks; first passage occurs at the first backward crossing of $z = 0$. The probability at the n_p -th peak is $P(n_p) = C_{n_p-1}/2^{2n_p-1}$, connecting to Spitzer’s identity [3] and Andersen’s equivalence principle [5].

2.2 Motzkin extension for forward scattering

Catalan numbers count Dyck paths—walks restricted to up- and down-steps. Forward scattering introduces flat steps (events preserving the sign of z -velocity), requiring the Motzkin extension [15, 16, 17].

Definition (Motzkin polynomial). The Motzkin polynomial of degree n is

$$M_n(t) = \sum_{k=0}^{\lfloor n/2 \rfloor} T(n, k) \cdot t^{n-2k} \quad (10)$$

where $T(n, k)$ are the Motzkin triangle coefficients [18]:

$$T(n, k) = \frac{n!}{(n - 2k)! k! (k + 1)!} \quad (11)$$

The one-dimensional first-return probability with forward scattering becomes equation (2), encoding three processes: up-steps (positive z -projection), down-steps (negative z -projection), and flat steps (zero z -projection change).

3 The Boundary Truncation Factor

The Motzkin framework applies to one-dimensional scattering. To use it for three-dimensional Henyey–Greenstein transport, we need a mapping—an effective backscattering coefficient $r_b(g, n)$ that makes the 1D formula reproduce 3D first-return probabilities. This section introduces the Boundary Truncation Factor (BTF), the correction that makes this mapping work.

3.1 Physical origin

In bulk scattering without boundaries, the effective asymmetry parameter after n scattering events follows standard multiple-scattering theory: $g_{\text{eff}}^{(\text{bulk})} = g^n$. Each scattering event multiplies the anisotropy, progressively randomizing the photon direction.

First-passage problems impose geometric constraints that modify this relationship. The requirement that photons return to their entry boundary restricts the accessible angular phase space: trajectories that wander too far forward are less likely to return. This geometric truncation accumulates over multiple scattering events, effectively reducing the asymmetry parameter beyond the bulk value:

$$g_{\text{eff}}^{(\text{constrained})} = g^n \cdot \text{BTF}(n, g) \quad (12)$$

where $\text{BTF} \leq 1$ represents the multiplicative reduction due to boundary constraints.

Formally, the BTF emerges from boundary-constrained angular integration:

$$g_{\text{eff}}^{(\text{constrained})} = \frac{\int \cdots \int \prod_{i=1}^n P_{\text{HG}}(\mu_i; g) \times [\text{return constraint}] \, d\mu_1 \cdots d\mu_n}{\int \cdots \int \prod_{i=1}^n P_{\text{HG}}(\mu_i; g) \, d\mu_1 \cdots d\mu_n} \quad (13)$$

where the constraint ensures the photon crosses below $z = 0$ after exactly n scattering events. These nested integrals become analytically intractable beyond $n = 3$.

3.2 Empirical discovery

Since direct evaluation of equation (13) is impractical, we determined BTF empirically. Monte Carlo simulations provide exact first-return probabilities for 3D photon transport. The computational campaign covered $g \in [0.05, 0.95]$ and $n \in [2, 100]$ with 10^8 trajectories per parameter combination—approximately 10^{12} total photon histories.

For each (g, n) pair, we extracted the BTF as the value needed to make the 1D Motzkin formula reproduce the Monte Carlo 3D result:

$$P_{\text{3D}}^{(\text{MC})}(n, g) = P_{\text{1D}}^{(\text{Motzkin})}(n, r_b(g, n)) \quad (14)$$

where $r_b(g, n)$ depends on BTF through the effective anisotropy.

3.3 The Cauchy kernel

Systematic model selection—starting with high-order Padé approximants and progressively reducing complexity while monitoring cross-validation error—revealed that the optimal functional form is a Cauchy kernel:

$$\text{BTF}(n, g) = \frac{A(g)}{1 + \left(\frac{n-2}{m_*(g)}\right)^2} \quad (15)$$

with parameters:

$$A(g) = 1 - \frac{g(1+g)}{2} = \frac{(1-g)(2+g)}{2} \quad (\text{amplitude}) \quad (16)$$

$$m_*(g) = \frac{4g}{1-g} \quad (\text{width}) \quad (17)$$

The peak location $n_0 = 2$ corresponds to the minimum scattering order for first return. This parameterized form reproduces Monte Carlo-derived BTF values with mean deviation <2% and cross-validated $R^2 > 0.999$ for $g \leq 2/3$.

Limiting behavior. For short paths ($n-2 \ll m_*$), $\text{BTF} \approx A(g)$ with minimal boundary effects. For long paths ($n-2 \gg m_*$), $\text{BTF} \rightarrow 0$ as boundary truncation dominates. At $g = 0$ (isotropic), $A = 1$ and $m_* = 0$, so $\text{BTF} = 1$ for $n = 2$ and $\text{BTF} = 0$ for $n > 2$ —reflecting that isotropic scattering requires exactly two steps for first return.

4 Monte Carlo procedure

This section details the Monte Carlo simulations from which the BTF was extracted.

4.1 Simulation procedure

First return occurs when z first becomes negative [19, 20]. The procedure:

1. Initialize photon at origin ($z = 0^+$), direction cosine $\mu_0 = 1$
2. For each scattering event:
 - Sample path length from $p(c) = e^{-c}$ (unit mean free path)
 - Sample scattering angle from HG phase function via inverse CDF
 - Update position; check if $z < 0$
3. Record scattering order n at first occurrence of $z < 0$
4. Repeat for 10^8 trajectories per (g, n) combination

The Henyey–Greenstein phase function is

$$P_{\text{HG}}(\mu; g) = \frac{1 - g^2}{2(1 + g^2 - 2g\mu)^{3/2}}, \quad -1 \leq \mu \leq 1 \quad (18)$$

where $g = \langle \mu \rangle \in [0, 1]$ is the anisotropy parameter.

4.2 Fit quality

Figure 1 compares Monte Carlo first-return probabilities with the BTF-corrected Motzkin theory. The Cauchy kernel captures the Monte Carlo data with mean deviation $< 2\%$ for $g < 2/3$.

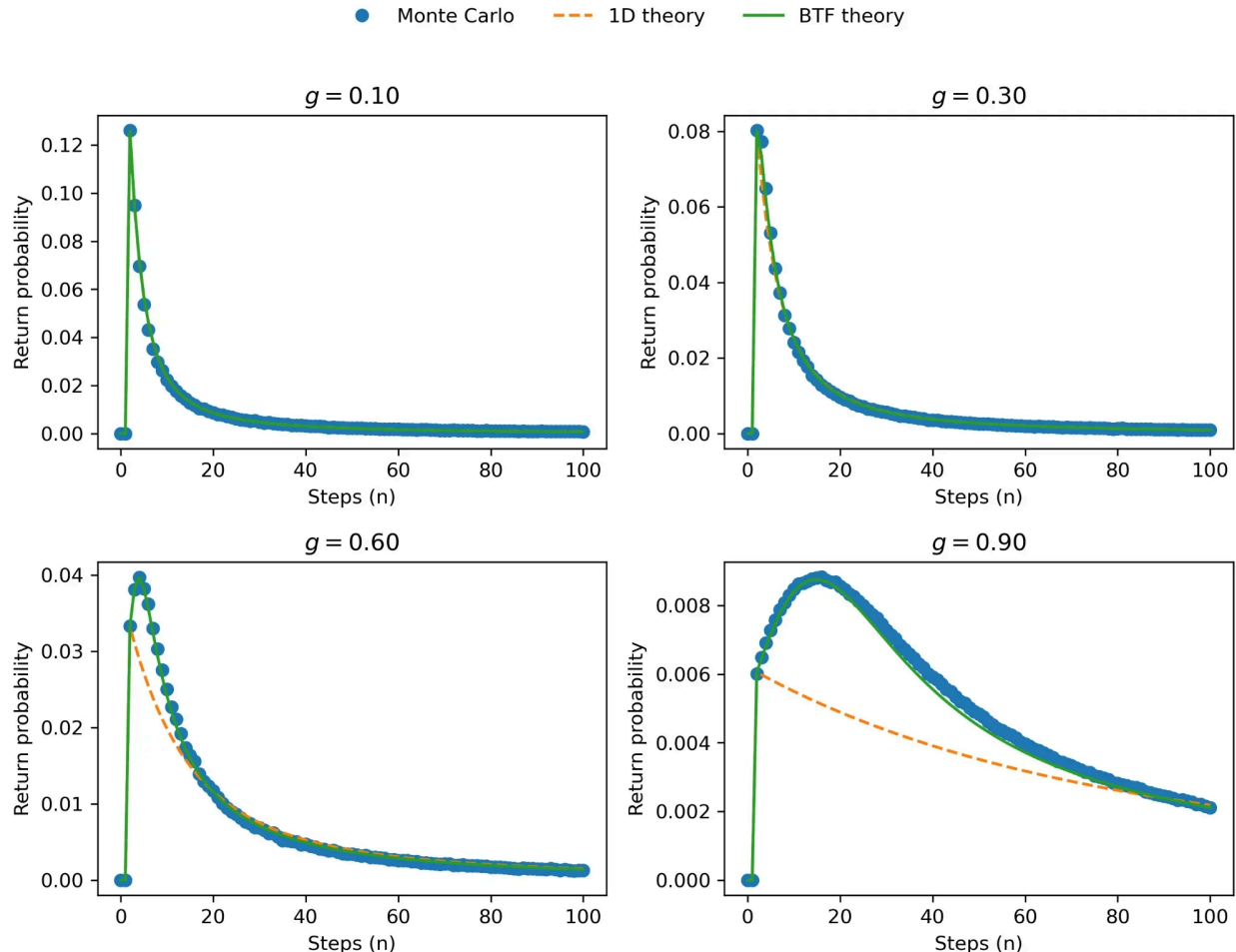


Figure 1: First-return probability versus scattering order n for $g = 0.10, 0.30, 0.60, 0.90$. Circles: Monte Carlo (10^8 trajectories). Dashed curves: 1D Motzkin formula without BTF correction. Solid curves: BTF-corrected formula. At $g = 0.90$, deviations appear near $n \approx 40$.

Error bounds. For $g < 2/3$, root-mean-square deviation is below 2% across all n . For $g > 2/3$, errors grow approximately as $\epsilon(g) \approx 0.05 \cdot (g - 2/3)/(1 - g)$, reaching $\sim 15\%$ at $g = 0.9$. For $g > 0.8$, the modified kernel (Section 7) is recommended.

5 Computational algorithm

We present the complete algorithm for mapping 3D Henyey–Greenstein scattering to 1D Motzkin combinatorics. The algorithm has four steps: (1) determine the angular threshold

separating forward from backward scattering; (2) compute the BTF-modified exponent; (3) evaluate the effective backscattering probability; (4) apply the Motzkin formula.

Step 1 (Angular threshold): The threshold $\mu_b(g)$ separates forward from backward hemispheres. Solve

$$p_{r2}(g) - \frac{1}{2}F(-\mu_b; g^2) = 0 \quad (19)$$

where $p_{r2}(g) = \int_{-1}^0 \frac{\mu' - 1}{\mu'} P_{\text{HG}}(\mu', g) d\mu'$ is the two-step return probability and $F(\cdot; g)$ is the HG cumulative distribution function.

Step 2 (Effective exponent): The BTF modifies how angular convolution accumulates with scattering order. The effective exponent

$$\gamma(g, n) = 2 + \text{BTF}(n, g)(n - 2) \quad (20)$$

interpolates between $\gamma = 2$ at $n = 2$ (minimum scattering order) and larger values as n increases.

Step 3 (Effective backscattering): Substitute into the HG CDF:

$$r_b(g, n) = F(-\mu_b(g); g^{\gamma(g, n)}) \quad (21)$$

Step 4 (First-return probability): The 3D first-return probability follows from equation (2) with the effective backscattering:

$$P_{\text{3D}}^{(\text{refl})}(g, n) = M_{n-2} \left(\frac{1 - 2r_b}{r_b} \right) \cdot \left(\frac{r_b}{2} \right)^{n-1} \quad (22)$$

This maps 3D Henyey–Greenstein scattering to 1D Motzkin combinatorics.

6 Oblique incidence: Motzkin extension

At oblique incidence, scattering events can redistribute momentum in the x - y plane without changing z . This transverse activity requires an extended Motzkin structure.

6.1 Physical motivation

At normal incidence ($\theta_0 = 0$), photons enter the medium traveling along the z -axis. The first-return problem depends only on the z -component of the random walk. Transverse motion in the x - y plane is integrated out, and the problem reduces to a one-dimensional Motzkin structure.

At oblique incidence ($\theta_0 \neq 0$), photons carry initial momentum in the transverse plane. Scattering events now partition into three categories:

1. **Backward steps** (n_p): direction reversals that change the sign of μ_z
2. **Forward-preserving flat steps** (n_f): scattering events that preserve $\mu_z > 0$ or $\mu_z < 0$
3. **Transverse flat steps** (n_{xy}): scattering events that primarily redistribute momentum in the x - y plane

Transverse activity n_{xy} vanishes at normal incidence but matters at oblique angles.

6.2 Combinatorial framework

We introduce the extended scattering order decomposition:

$$m_s = 2n_p + n_f + n_{xy} \quad (23)$$

where m_s is the total number of scattering events, n_p counts peaks (direction reversals), n_f counts forward-preserving flat steps, and n_{xy} counts transverse flat steps.

The step probabilities satisfy the normalization constraint:

$$r_b + r_f + r_{xy} = 1 \quad (24)$$

where $r_b(\theta_0, g)$ is the backscattering probability, $r_f(\theta_0, g)$ is the forward-flat probability, and $r_{xy}(\theta_0, g)$ is the transverse probability.

At normal incidence: $r_{xy} = 0$, $r_f = 1 - r_b$, and the structure collapses to the standard Motzkin form.

6.3 Full marginal probability

Summing over all possible transverse activities yields the probability of first return at scattering order m_s :

$$P_{3D}^{\text{marg}}(m_s; r_b, r_{xy}) = \sum_{n_{xy}=0}^{m_s-2} \sum_{n_p=1}^{\lfloor (m_s-n_{xy})/2 \rfloor} \left(\frac{1}{2^{2n_p-1}} \cdot \frac{(m_s-2)!}{(m_s-n_{xy}-2n_p)! n_{xy}! n_p! (n_p-1)!} \right. \\ \left. \times r_b^{2n_p-1} \cdot r_{xy}^{n_{xy}} \cdot (1-r_b-r_{xy})^{m_s-n_{xy}-2n_p} \right) \quad (25)$$

This is the extended Motzkin representation for oblique incidence.

6.4 Reduction to normal incidence

Proposition (Normal incidence reduction). At normal incidence ($r_{xy} = 0$, $n_{xy} = 0$), the 3D marginal probability reduces exactly to the 1D marginal:

$$P_{3D}^{\text{marg}}(m_s; r_b, 0) = P_{1D}^{\text{marg}}(m_s; r_b) \quad (26)$$

Proof. Setting $r_{xy} = 0$ forces $n_{xy} = 0$. The double sum collapses to a single sum over n_p , recovering equation (2). \square

The extension properly generalizes the standard theory.

Remark (Monte Carlo scope). The Monte Carlo validation in Section 4 addresses normal incidence only. Monte Carlo calibration at oblique incidence remains for future work.

7 High-anisotropy extension: Modified Cauchy kernel

The Cauchy BTF derived in Section 3.3 works to 2% for $g < 2/3$. Biological tissue has $g \approx 0.9\text{--}0.98$ [21, 22], outside this range. Here we develop a one-parameter extension that reduces errors by roughly half at high g .

7.1 Systematic deviations at high g

The 10^{12} photon data show systematic deviations from Cauchy at high g . Figure 2 plots $(P_{\text{MC}} - P_{\text{Cauchy}})/P_{\text{Cauchy}}$ against $(n - 2)/m_x$: for $g > 0.85$, Monte Carlo runs high near the peak and low in the tail—lighter tails than Cauchy.

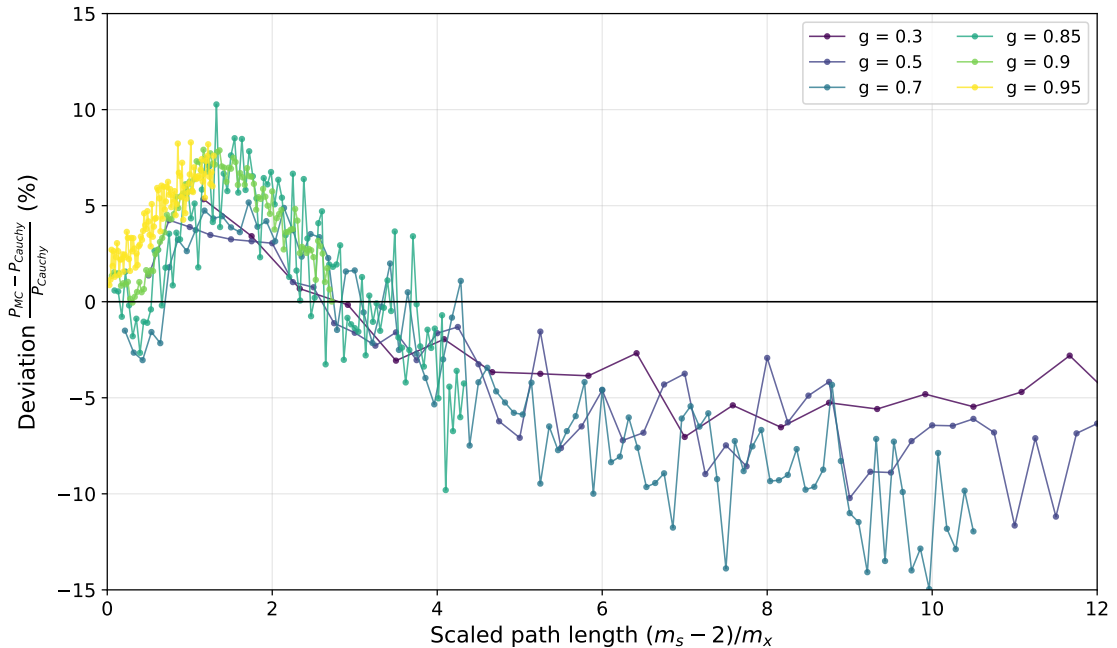


Figure 2: Deviations from the Cauchy kernel versus scaled path length. At high g , Monte Carlo runs high near the peak and low in the tail—the signature of lighter-than-Cauchy tails.

7.2 Modified Cauchy kernel

The generalization lets the exponent vary:

$$K_\alpha(x) = \frac{1}{[1 + x^2]^{(1+\alpha)/2}} \quad (27)$$

with shape parameter α . Setting $\alpha = 1$ recovers Cauchy; $\alpha > 1$ gives faster tail decay. This “generalized Cauchy” appears in robust statistics [24, 25]. Note that α is a shape parameter, not a Lévy stability index.

The modified BTF becomes

$$\text{BTF}_\alpha(n, g) = \frac{A(g)}{\left[1 + \left(\frac{n-2}{m_*(g)}\right)^2\right]^{(1+\alpha(g))/2}} \quad (28)$$

with $A(g)$ and $m_*(g)$ unchanged.

7.3 Fitting the shape parameter

We fit α at each g by least squares against Monte Carlo. The results follow

$$\alpha(g) = 1 + \frac{g - \frac{2}{3}}{30(1-g)} \quad (29)$$

Table 4 compares fitted and calculated values. The parameter stays close to unity: $\alpha \approx 0.98$ at low g , rising to $\alpha \approx 1.2$ at $g = 0.95$.

Table 4: Fitted α versus formula (29).

g	m_*	α (fitted)	α (formula)	$(1 + \alpha)/2$
0.10	0.4	0.981	0.979	0.99
0.30	1.7	0.990	0.983	0.99
0.50	4.0	0.990	0.989	0.99
$\frac{2}{3}$	8.0	—	1.000	1.00
0.80	16	1.018	1.022	1.01
0.90	36	1.090	1.078	1.04
0.95	76	1.196	1.189	1.09

Figure 3 plots $\alpha(g)$ over the full range. The crossover $\alpha = 1$ occurs at $g = 2/3$, where the Cauchy BTF begins to deviate.

The formula contains the factor $1/(1-g) = \ell^*/\ell$, the transport-to-scattering mean free path ratio. Figure 4 replots α against this variable; $\alpha = 1$ occurs at $\ell^*/\ell = 3$.

We stress that equation (29) is an empirical fit, not a derivation. It minimizes squared error across all n and captures the trend, but the factor of 30 lacks theoretical explanation.

7.4 Practical recommendations

Guidelines for implementation:

- $g < 0.85$: use the standard Cauchy BTF. Errors remain under 2%, and the formula is simpler.
- $0.85 \leq g \leq 0.95$: use the modified form with α from equation (29). RMSE improves by $\sim 45\%$.

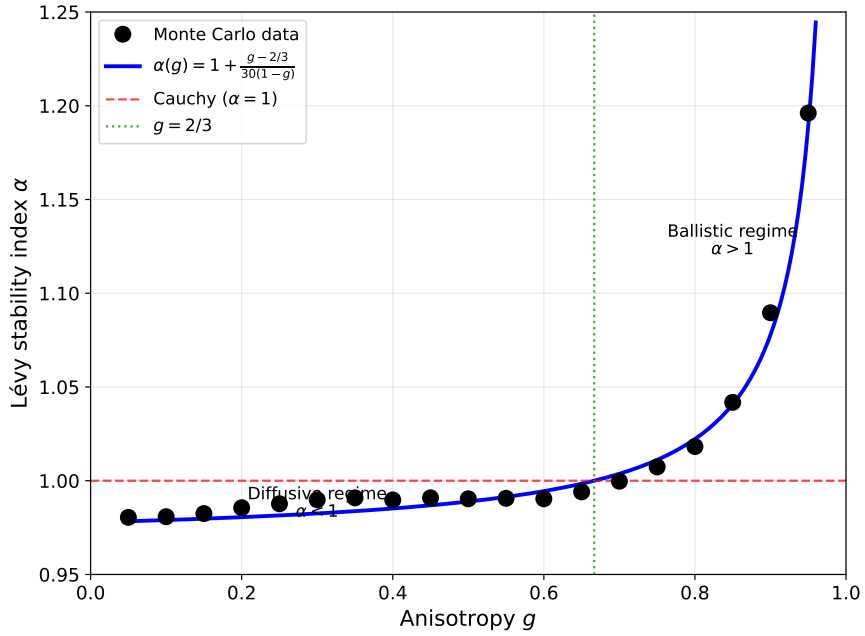


Figure 3: Shape parameter α versus anisotropy g . Solid curve: equation (29). Dashed line: $\alpha = 1$ (standard Cauchy). The crossover at $g = 2/3$ separates the diffusive regime ($\alpha < 1$) from the ballistic regime ($\alpha > 1$).

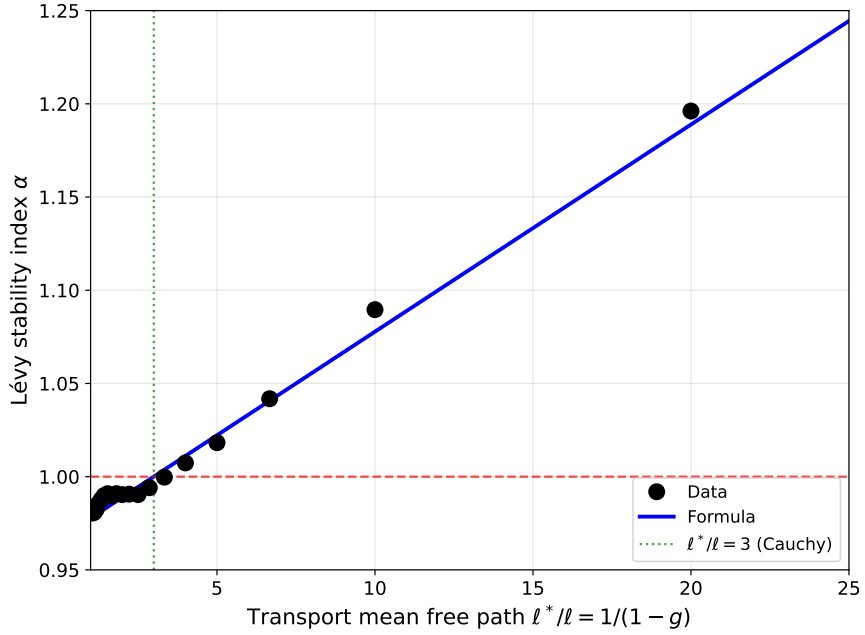


Figure 4: Shape parameter α versus transport mean free path ratio $\ell^*/\ell = 1/(1-g)$. The Cauchy case $\alpha = 1$ occurs at $\ell^*/\ell = 3$.

- $g > 0.95$: the formula has not been validated beyond $g = 0.95$. Monte Carlo calibration is recommended.

For tissue optics ($g \approx 0.9$ – 0.95), the modified kernel extends the analytical BTF into the regime of primary interest.

8 Conclusions

We have shown that first-return statistics in three-dimensional Henyey–Greenstein scattering can be captured by a simple and highly constrained Boundary Truncation Factor that corrects the one-dimensional Motzkin framework for boundary-induced angular filtering. Monte Carlo simulations over a broad parameter space demonstrate that this factor follows a Cauchy kernel in the scattering order, with parameters determined solely by the anisotropy factor g . The accuracy and parsimony of the result are notable: a small number of parameters captures the full dependence on scattering order and anisotropy with percent-level fidelity for $g < 2/3$.

For higher anisotropy, where deviations from the pure Cauchy form emerge, a one-parameter generalization preserves the kernel structure while significantly reducing error. The resulting framework replaces large-scale three-dimensional Monte Carlo simulations with one-dimensional polynomial evaluation, enabling substantial computational savings in inverse problems and parameter studies.

The emergence of a Cauchy kernel from boundary-constrained three-dimensional transport is robust but not yet theoretically explained. The appearance of simple integer coefficients in the kernel parameters suggests that a deeper geometric or first-passage-theoretic derivation may exist. Establishing such a derivation, and extending the present framework to oblique incidence and more general geometries, remain important directions for future work.

Acknowledgements

CZ thanks Dr. Florence Zeller for discussions on Chebyshev polynomials and Motzkin structures, Professor Arnold Kim for encouragement and guidance, and Professor Michel Talagrand for perspective on the difficulty of proving the Cauchy kernel rigorously. The authors used AI tools (Claude, Anthropic) for editorial assistance; all scientific content, derivations, and interpretations are the authors' own.

A Notation summary

Table 5 summarizes the notation.

Table 5: Principal notation.

Symbol	Definition	Notes
<i>Scattering parameters</i>		
g	$\langle \cos \theta \rangle$	Anisotropy factor, $g \in [0, 1)$
μ	$\cos \theta$	Direction cosine
$P_{\text{HG}}(\mu; g)$	equation (18)	Henyey–Greenstein phase function
S	scattering coefficient	Units: inverse length
χ	absorption coefficient	Units: inverse length
<i>Random walk quantities</i>		
n	scattering order	Number of scattering events
m_s	total scattering order	$= 2n_p + n_f + n_{xy}$
n_p	peak count	Direction reversals
n_f	forward-flat count	Forward-preserving flat steps
n_{xy}	transverse count	Transverse flat steps
c	path length	Between successive scattering events
<i>Step probabilities</i>		
r_b	backscattering probability	$3D \rightarrow 1D$ mapped parameter
r_f	forward-flat probability	Forward-preserving step
r_{xy}	transverse probability	Transverse step; $= 0$ at normal incidence
r	backward-step probability	1D model parameter
<i>BTF parameters</i>		
BTF	Boundary Truncation Factor	Equation (3)
$A(g)$	amplitude	$1 - g(1 + g)/2$
$m_*(g)$	width parameter	$4g/(1 - g)$
n_0	peak location	$= 2$ (minimum scattering order for return)
$\alpha(g)$	shape parameter	$1 + (g - 2/3)/[30(1 - g)]$; equation (29)
<i>Combinatorial objects</i>		
C_n	Catalan number	$(2n)!/(n!(n + 1)!)$
$M_n(t)$	Motzkin polynomial	Equation (10)
$T(n, k)$	Motzkin triangle coefficient	$n!/((n - 2k)! k! (k + 1)!)$

References

- [1] Redner S 2001 *A Guide to First-Passage Processes* (Cambridge: Cambridge University Press)
- [2] Rudnick J and Gaspari G 2004 *Elements of the Random Walk* (Cambridge: Cambridge University Press)
- [3] Spitzer F 1964 *Principles of Random Walk* (New York: Springer)
- [4] Feller W 1971 *An Introduction to Probability Theory and Its Applications* vol 2, 2nd edn (New York: Wiley)
- [5] Andersen E S 1962 The equivalence principle in the theory of fluctuations of sums of random variables *Colloquium on Combinatorial Methods in Probability Theory, Aarhus* pp 13–16
- [6] Zeller C and Cordery R 2020 Light scattering as a Poisson process and first-passage probability *J. Stat. Mech.* **2020** 063404
- [7] Zeller C and Cordery R 2024 First-return statistics in bounded radiative transport: A Motzkin polynomial framework *Preprint* arXiv:2512.13986
- [8] Kubelka P and Munk F 1931 *Z. Tech. Phys.* **12** 593–601
- [9] Chandrasekhar S 1960 *Radiative Transfer* (New York: Dover)
- [10] Sandoval C and Kim A D 2014 Deriving Kubelka–Munk theory from radiative transport *J. Opt. Soc. Am. A* **31** 628–636
- [11] Sandoval C and Kim A D 2017 Generalized Kubelka–Munk approximation for multiple scattering of polarized light *J. Opt. Soc. Am. A* **34** 153–162
- [12] Myrick M L, Simcock M N, Baranowski M, Brooke H, Morgan S L and McCutcheon J N 2011 The Kubelka–Munk diffuse reflectance formula revisited *Appl. Spectrosc. Rev.* **46** 140–165
- [13] Henyey L G and Greenstein J L 1941 Diffuse radiation in the galaxy *Astrophys. J.* **93** 70–83
- [14] Pfeiffer N and Chapman G H 2008 Successive order, multiple scattering of two-term Henyey–Greenstein phase functions *Opt. Express* **16** 13637–13645
- [15] Oste R and Van der Jeugt J 2015 Motzkin paths, Motzkin polynomials and recurrence relations *Electron. J. Combin.* **22**(2) P2.8
- [16] Drake D and Gantner R 2011 Generating functions for plateaus in Motzkin paths *Preprint* arXiv:1109.3272

- [17] Simon K and Trachsler B 2003 A random walk approach for light scattering in material *Discrete Math. Theor. Comput. Sci.* pp 289–300
- [18] Sloane N J A 2023 A handbook of integer sequences fifty years later *Preprint* arXiv:2301.03149
- [19] Jacques S L 2010 Monte Carlo modeling of light transport in tissue (steady state and time of flight) *Optical-Thermal Response of Laser-Irradiated Tissue* 2nd edn (Berlin: Springer) pp 109–144
- [20] Sassaroli A, Blumetti C, Martelli F, Alianelli L, Contini D, Ismaelli A and Zaccanti G 1998 Monte Carlo procedure for investigating light propagation and imaging of highly scattering media *Appl. Opt.* **37** 7392–7400
- [21] Jacques S L 2013 Optical properties of biological tissues: a review *Phys. Med. Biol.* **58** R37–R61
- [22] Binzoni T, Leung T S, Gandjbakhche A H, Rüfenacht D and Delpy D T 2006 The use of the Henyey–Greenstein phase function in Monte Carlo simulations in biomedical optics *Phys. Med. Biol.* **51** N313–N322
- [23] Modrić D, Bolanča S and Beuc R 2009 Monte Carlo modeling of light scattering in paper *J. Imaging Sci. Technol.* **53** 020201
- [24] Carrillo R E, Aysal T C and Barner K E 2010 A generalized Cauchy distribution framework for problems requiring robust behavior *EURASIP J. Adv. Signal Process.* **2010** 312989 (pp 1–17)
- [25] Alzaatreh A, Lee C, Famoye F and Ghosh I 2016 The generalized Cauchy family of distributions with applications *J. Stat. Distrib. App.* **3** 12 (pp 1–16)